© 2017. Published by The Company of Biologists Ltd | Journal of Experimental Biology (2017) 220, 3499-3507 doi:10.1242/jeb.159376

RESEARCH ARTICLE

Role of outstretched forelegs of flying beetles revealed and demonstrated by remote leg stimulation in free flight

Yao Li, Feng Cao, Tat Thang Vo Doan and Hirotaka Sato*

ABSTRACT

In flight, many insects fold their forelegs tightly close to the body, which naturally decreases drag or air resistance. However, flying beetles stretch out their forelegs for some reason. Why do they adopt this posture in flight? Here, we show the role of the stretched forelegs in flight of the beetle *Mecynorrhina torquata*. Using leg motion tracking and electromyography in flight, we found that the forelegs were voluntarily swung clockwise in yaw to induce counter-clockwise rotation of the body for turning left, and vice versa. Furthermore, we demonstrated remote control of left–right turnings in flight by swinging the forelegs via a remote electrical stimulator for the leg muscles. The results and demonstration reveal that the beetle's forelegs play a supplemental role in directional steering during flight.

KEY WORDS: Insect flight, Neuromuscular stimulation, Leg swing, Remote radio control, Physiology, Electromyography

INTRODUCTION

The flight posture of many insects, including butterflies, locusts, dragonflies, moths and bees, is commonly described as the legs being folded or pressed closely against the body during flight (Borst, 1986; Burrows, 1996; Nachtigall, 1974). In contrast, beetles fully lift and outstretch their forelegs while inflight (Fig. 1). Moreover, many beetle species have thick, long forelegs, unlike most flying insects (Van Truong et al., 2014). Naively, flying with outstretched legs would seem inadvisable, as it would tend to increase drag (Combes and Dudley, 2009). Meanwhile, beetles often swing their forelegs while inflight. According to the physical principle of conservation of angular momentum, when a leg rotates (swings) about the leg base (coxa), the body of the flying beetle should rotate in the opposite direction (Mountcastle et al., 2015). A long and relatively heavy foreleg will have a relatively large moment of inertia so that the resulting torque exerted on the body might be large enough to significantly rotate the body inflight.

As reported in many insect species, body structures apart from the wings could also contribute to the flight control, and function as auxiliary maneuvers (Wagner, 1986; Taylor and Thomas, 2003; Camhi, 1970; Rowell, 1988; Zanker et al., 1991). Specifically, it is reported that both the abdomen and the hindlegs of the locust are effective in assisting with flight turnings and compensating for flight fluctuations by swaying them laterally (Camhi, 1970; Rowell, 1988; Arbas, 1986). Similarly, Zanker (1988) demonstrated by visual stimulation that the abdomen of flies takes an active role in flight directional control. The honeybee widely manipulates its body streamline to adjust the flying speeds and heading directions (Luu et al., 2011; Nachtigall, 1974). Meanwhile, the bees make use of their hindlegs to stabilize their body in flight (Combes and Dudley, 2009; Mountcastle et al., 2015). It has also been found that the elytra of beetles are placed asymmetrically in flight turnings to produce uneven lift (Van Truong et al., 2012). Even the rotation of the head has been found to visually coordinate the flight turnings in locusts (Hensler and Robert, 1990; Miall, 1990). We believe the stable and efficient flight of insects cannot be separated from the diverse auxiliary maneuvers.

Here we show that the forelegs are 'intentionally' outstretched and swung to facilitate turning while inflight. The beetle turns its body (the direction of propulsion) by swinging its forelegs. Leg motion tracking and electromyography (EMG) in tethered flight showed that the forelegs were voluntarily swung clockwise in yaw to induce counter-clockwise rotation of the beetle body for left turning, and vice versa. The yaw torque generated by leg swing was measured, which was proved large enough to rotate the body. Furthermore, we demonstrated remote control of left–right turnings in flight by swinging the forelegs via a remote electrical stimulator. As the wings are the dominant mechanism for controlling insect flight (Chapman et al., 2012), the present study indicates that the outstretched foreleg plays a supplemental role in steering during flight.

MATERIALS AND METHODS

Animals

The animals used in this study were adult male *Mecynorrhina torquata* (Drury 1782) beetles (order Coleoptera; length: 62±8 mm; mass: 7.4±1.3 g) that were fed with beetle jellies twice a week. The rearing room was maintained at a temperature and humidity of approximately 25°C and 60%, respectively. Beetles that could fly freely for more than 10 s were selected for the experiments. The use of this animal was permitted by the Agri-Food and Veterinary Authority of Singapore (AVA; HS code: 01069000, product code: ALV002). Invertebrates, including beetles, are exempt from ethics approval for animal experiments according to the National Advisory Committee for Laboratory Animal Research (NACLAR) guidelines.

Electrode implantation

Each beetle was anesthetized in a small sealed bag containing CO_2 for 1 min. Next, the legs were constrained by a rubber band. Two tiny holes were pierced through the cuticle above the target muscle using insect pins (enamel-coated #5, Indigo Instruments, Waterloo, ON, Canada). The electrodes consisted of 10-cm segmented Teflon-insulated silver wires (127 µm uncoated diameter, 178 µm coated diameter; A-M Systems, Sequim, WA, USA). One side of the silver wire was flamed to remove the insulated layer and expose the silver layer. The flamed ends were inserted through the tiny holes to a depth of approximately 3 mm. Melted beeswax was used to cover

School of Mechanical and Aerospace Engineering, Nanyang Technological University, Singapore 639798, Singapore.

*Author for correspondence (hirosato@ntu.edu.sg)

H.S., 0000-0003-4634-1639

Received 29 March 2017; Accepted 24 July 2017

Journal of Experimental Biology (2017) 220, 3499-3507 doi:10.1242/jeb.159376

Fig. 1. Inflight postures of the beetle *Mecynorrhina torquata* (top left), the butterfly *Leptidea amurensis* (top right), the dragonfly *Anax parthenope* (bottom left) and the honey bee *Apis mellifera* (bottom right). The flying beetles always outstretch their forelegs (Van Truong et al., 2014), whereas other insects tend to fold or press their forelegs closely against the body during flight (Borst, 1986; Burrows, 1996; Nachtigall, 1974). Photo credit (except top left): Kazuo Unno.

the holes because beeswax quickly solidifies and thus immobilizes the silver wires.

Leg motion tracking under visual stimulation

As demonstrated in previous studies, visual stimulation (optical flow of dark and bright stripes) can induce fictive turnings in flying insects (Götz and Wenking, 1973; Luu et al., 2011; Zanker, 1988); thus, we chose this type of visual stimulation to determine the steering ability of beetle forelegs. The beetle was tethered to constrain its flight within the range of a universal coupler (Fig. S1). Thus, the beetle was capable of rolling or pitching its body, but yaw rotation was restricted. The beetle was placed ∼20 cm in front of a translucent screen, which was used for projecting the wide-field optical flow patterns (dark and bright stripes) that moved leftward or rightward (Sato et al., 2015). The stripes are 35 mm in width with a contrast rate of 2.5 Hz. In left stimulations, the stripes were moving from right to left and induced leftward turnings, and vice versa. Both left and right visual stimulations lasted 10 s, and the presentation of the two stimulations was alternated. There was a 5 s interval between the stimulations. Thus, one complete visual cycle lasted 30 s.

To track the locomotion of both forelegs, three retro-reflective markers were placed on the beetle, and a referential marker was placed at the rotation center of the coupler. As shown in Fig. S1, one marker was placed at the posterior end of the pronotum and the other two markers were placed at the tips of both foreleg tibias. Moreover, the distances between the foreleg coxae and pronotum marker were measured. A motion capture system (Vicon, Oxford, UK) consisting of six T40s cameras with a resolution of 4 megapixels (2336×1728 pixels) was used to detect the 3D coordinates of the markers by tracking the retro-reflective markers (Manecy et al., 2015; Thies et al., 2007). The coordinates exported from Vicon were recorded at 150 Hz and synchronized with the visual stimulation.

The effects of the visual stimulations were assessed by analyzing the lateral movement of the pronotum marker. When the beetle needs to roll its body toward the turning direction, it will swing the free end of the coupler as the coupler is always perpendicular to the body. Then the free end of the coupler will be swung at the same angle as roll around the center of the coupler, which will move the beetle laterally in the opposite direction of turning. Thus, the visual stimulation was effective when the pronotum marker shifted to the opposite side from the direction of stimulation. All data were extracted from the period when the stimulation was effective. The coordinate system for the calculation was based on the beetle body, which defined the heading direction as the x-axis and a plane parallel to the body-neutral surface as the X–Y plane (Wang et al., 2003). A coordinate transformation was required because the raw data from Vicon were based on a geodetic coordinate system. The origins of the geodetic coordinate system and body coordinate system were both set at the referential marker. Yaw rotation was constrained in the experiment; thus, the derived equation of a spatial coordinate transformation was expressed as follows:

$$\begin{bmatrix} \mathbf{X}' \\ \mathbf{Y}' \\ \mathbf{Z}' \end{bmatrix} = \mathbf{R}_x(\varepsilon_x) \cdot \mathbf{R}_y(\varepsilon_y) \cdot \begin{bmatrix} \mathbf{X} \\ \mathbf{Y} \\ \mathbf{Z} \end{bmatrix} = \begin{bmatrix} \cos\varepsilon_y & 0 & -\sin\varepsilon_y \\ \sin\varepsilon_x \sin\varepsilon_y & \cos\varepsilon_x & \sin\varepsilon_x \cos\varepsilon_y \\ \cos\varepsilon_x \sin\varepsilon_y & -\sin\varepsilon_x & \cos\varepsilon_x \cos\varepsilon_y \end{bmatrix} \cdot \begin{bmatrix} \mathbf{X} \\ \mathbf{Y} \\ \mathbf{Z} \end{bmatrix}. \quad (1)$$

$[\mathbf{X}'\ \mathbf{Y}'\ \mathbf{Z}']^{\mathrm{T}}$ and $[\mathbf{X}\ \mathbf{Y}\ \mathbf{Z}]^{\mathrm{T}}$ are the coordinates in the transformed body system and original geodetic system, respectively. $\mathbf{R}_x$ and $\mathbf{R}_y$ are the rotation matrixes for the x-axis and y-axis, respectively. Angles ε_x and ε_y are the rotation angles around the x-axis (roll) and y-axis (pitch) that were obtained through the vector pointing from the pronotum marker to the referential marker in the geodetic coordinate system. The angular displacement of the leg was defined as the angle between the heading direction and the leg vector pointing from the coxa to the tibia on the body's coordinate system (Fig. 2A). The swing direction of the left (right) foreleg was determined to be clockwise (counterclockwise) when the average angular displacement of the stimulation decreased from the average angular displacement of the stimulation right before it, and vice versa. All of the angular displacements discussed herein refer to their absolute values.

EMG measurement

EMG measurement was conducted under visual stimulation. Two silver wires were implanted into the tissue of the target muscle to collect muscular potentials (unilateral EMG) during tethered flight

Journal of Experimental Biology (2017) 220, 3499-3507 doi:10.1242/jeb.159376

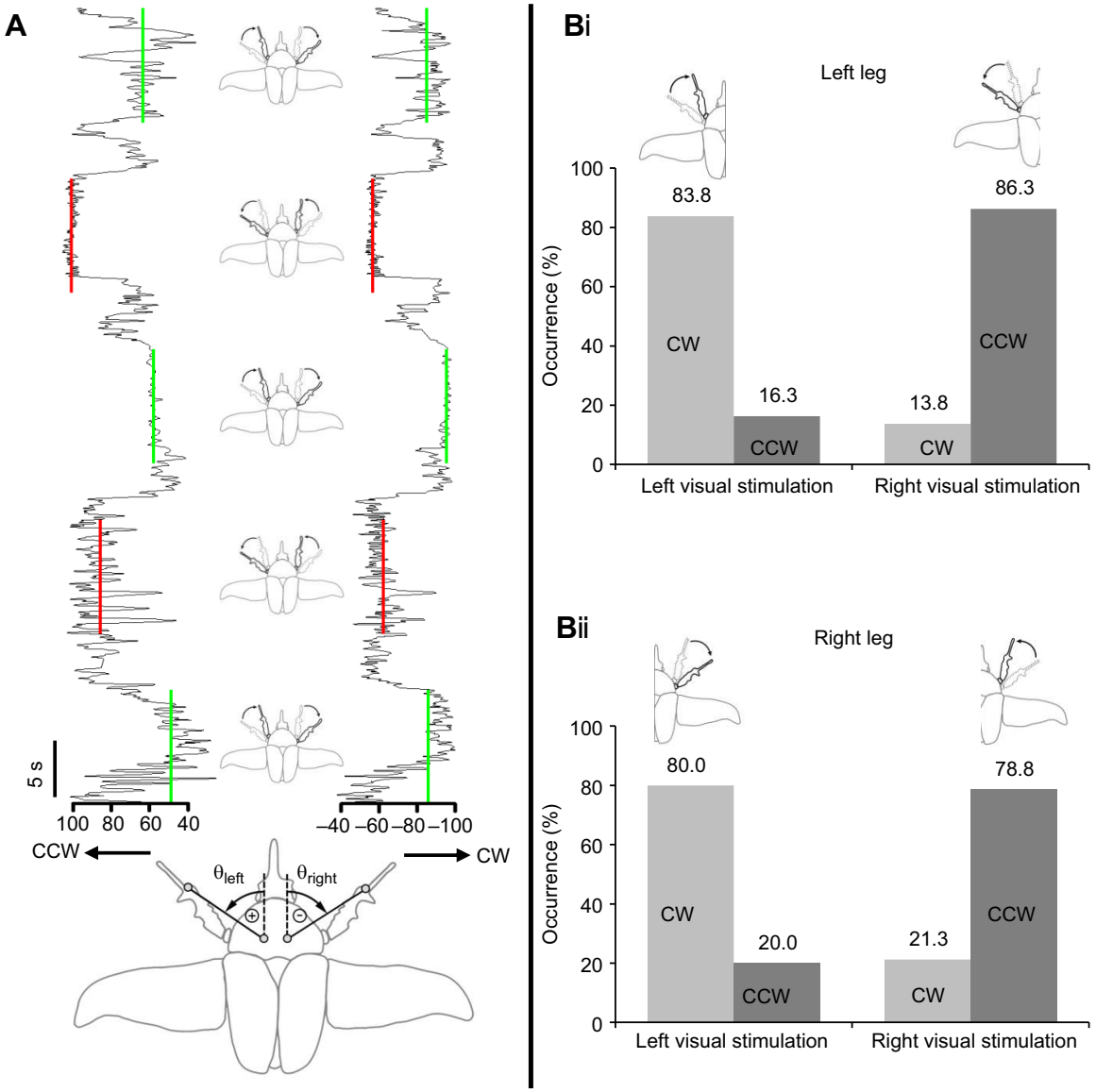

Fig. 2. Angular displacement of forelegs in response to visual stimulation. (A) Representative angular displacements were synchronized with visual stimulations. The black lines show the angular displacements of the left and right legs (θ_{left} and θ_{right}). The green and red bars show the average angular displacement in response to left and right visual stimulation, respectively. The length of the bars indicates the stimulation period. During left stimulation, the left leg moved closer to the body and the right leg moved away from the body (clockwise). During right stimulation, both legs moved in the opposite direction (counterclockwise). (B) The occurrence rates of clockwise (CW) and counterclockwise (CCW) swings were determined for both forelegs (N=10 beetles, n=80 left stimulations, n=80 right stimulations). The swing direction was determined by comparing the average angular displacement with the value for the former stimulation. The left leg (Bi) and right leg (Bii) moved clockwise at 83.8% and 80.0%, respectively, during left stimulation, whereas they moved counterclockwise at 86.3% and 78.8%, respectively, during right stimulation. All clockwise and counterclockwise rates showed a significant difference from chance level (P<0.0001, binomial test). See Movie 1.

(Sato et al., 2015). To avoid collision with the wings, the wires were spread along the coupler. The two non-implanted ends of silver wires were connected to the input of a signal amplifier (LT1920, Linear Technology Corporation, Milpitas, CA, USA) using alligator clips. The amplified signal was transmitted to a microcontroller-based (CC2430, 7×7 mm^2, 130 mg, 32 MHz clock, 2.4 GHz IEEE802.15.4-compliant RF transceiver, Texas Instruments, Dallas, TX, USA) development board (SOC_BB 1.1 and CC2430EM 1.2, Chipcon AS, Oslo, Norway). Using the A/D converter on the microcontroller, the collected data were digitalized for wireless transmission based on the IEEE 802.15.4 protocol. The EMG signal of the left protraction muscle was measured and analyzed (Fig. 3A). To avoid possible interference, the right protraction muscle was also implanted with silver wires. The recorded electrical signals were processed by a custom program. The EMG spikes were selected based on 5-sigma control limits and synchronized with visual stimulations. Specifically, the EMG spikes that occurred during the left and right visual stimulations and intervals without stimulation were assigned to their corresponding groups to compare the occurrence rate.

Torque measurement

Torque measurements of the body were collected with a torque sensor (Nano17 Titanium, ATI Industrial Automation, Apex, NC, USA) in tethered condition (Taylor and Thomas, 2003). The sensor was fixed vertically downward to the ground, and a custom holder

Journal of Experimental Biology (2017) 220, 3499-3507 doi:10.1242/jeb.159376

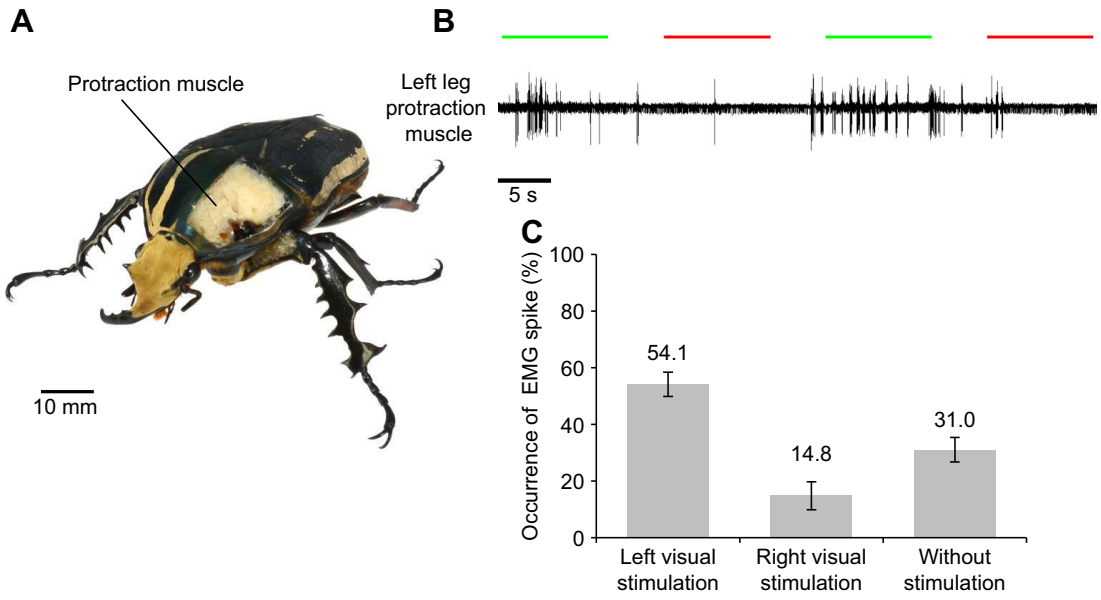

Fig. 3. Electromyography (EMG) measurements of the protraction muscle of the left foreleg. (A) Anatomical view of the left leg protraction muscle. (B) Representative EMG from protraction muscle during tethered flight. The recorded signals were synchronized with visual stimulation. The green and red bars indicate the periods of left and right visual stimulation, respectively. (C) The occurrence rate of EMG spikes during visual stimulation was determined (N=5 beetles, n=5 EMG recordings). In the protraction muscle, 54.1% of the spikes occurred during left visual stimulation, whereas only 14.8% occurred during right visual stimulation, which demonstrates the spikes occurred at higher rates under left stimulation (t_4=10.82, P=0.0002, t-test) and lower rates under right stimulation (t_4=8.44, P=0.0006, t-test). Error bars represent ±s.e.m.

was connected right below the sensor. The holder was designed to suspend the beetle at its pronotum. The z-axis of the coordinate system was vertically upward while the x-axis and y-axis were pointing forward and leftward, respectively. As measured with the inertia sensor and the method proposed by Li et al. (2016), the pitch angle of beetle body in flight was 28.38±3.65 deg (N=5 beetles, n=25 flights; all data are represented as means±s.d.). Thus, we adjusted the pitch angle of tethered beetle to 28 deg. The beetle was stuck to the holder by beeswax and two thin silver wires were implanted into the left foreleg protraction muscle. The two non-implanted ends of silver wires were connected to the output port of a function generator (33220A, Agilent Technologies, Santa Clara, CA, USA) using alligator clips. Prior to stimulation, the left foreleg was forcibly spread out to its flight position.

Leg motions were elicited with the monophasic square pulses from the function generator (0.7 V amplitude, 100 Hz frequency, 10% duty cycle and 500 ms duration). By applying the electrical signals from the function generator, the torque data were recorded with a sampling rate of 1000 Hz. The induced torque on the body, which was defined as the change in torque after stimulation, was extracted after synchronizing the torque data with electrical stimulations. Ten stimulations were conducted on each intact beetle, which means that all of the legs functioned normally. Ten additional stimulations were applied after leg amputation (i.e. the left foreleg was separated from its coxa) as a control group. Moreover, we scanned the legs, pronotum, abdomen and elytra of a beetle with a commercial 3D scanner (EinScan-Pro, Shining 3D, Hangzhou, China; 0.05 mm accuracy). The scanned point-cloud model was imported into a 3D modeling program (SolidWorks 2016, Dassault Systemes, Vélizy-Villacoublay, France) and the model was split into parallel layers in 1 mm spacing. A digital model was built by lofting the cross-sections of the layers (Fig. S2). We measured the mass of each part of the beetle and input the average masses into the digital model (N=5 beetles). Then we rotated the model 28 deg along the pitch axis to match the real flight orientation. The moment of inertia was calculated by the software. As torque equals to the product of moment of inertia and angular acceleration, the relationship between the rotation of body θ_{body} and the torque induced by leg motion T_{leg} is as follows:

$$\theta_{body} = \int \omega_{body} = \iint \alpha_{body} = \frac{\iint T_{leg}}{I_{body}}, \quad (2)$$

where ω_{body}, α_{body} and I_{body} are the angular velocity, angular acceleration and moment of inertia of the beetle body, respectively.

Wireless backpack assembly

The free-flight experiment was completed in a motion capture laboratory (dimension: 16×8×4 m). The laboratory was equipped with a motion capture system (Vicon) containing twenty T40 s and T160 cameras fixed along the upper edge of the room (Fig. S3B). The custom-made computer software (BeetleBrain v.0.99b) was used to generate signal commands via a guidance and inertial navigation assistant (GINA, provided by Professor Kris Pister's laboratory at the University of California, Berkeley) base station (2.4 GHz IEEE 802.15.4 wireless protocol). The commands were received and processed by an electrical wireless backpack described by Sato et al. (2015). Electrical signals were generated using two independent channels into the left and right protraction muscles. Each muscle was implanted with a pair of silver electrodes including a working electrode and a counter electrode. The muscles were unilaterally stimulated in the experiment. A rechargeable lithium ion battery (3.7 V, 350 mg, 8.5 mAh; Micro Avionics, Horsely, Derbyshire, UK) was connected to the backpack, and the surface was wrapped with retro-reflective tape (Silver-White, Reflexite Corporation, Oranienburg, Germany). The backpack assembly was attached to the pronotum of the beetle to enable the detection of 3D flight trajectories using the motion capture system (Fig. S3A).

Electrical stimulation in free flight

In the free-flying experiments, the backpack assembly was used to stimulate both foreleg protraction muscles. The electrical stimulation of the left or right protraction muscle induced the swing of the corresponding leg clockwise or counterclockwise (viewed from the dorsal side of the beetle). A preliminary experiment was conducted to determine the appropriate stimulation voltage for the protraction muscle. The function generator was used as the signal source, which generated pulse signals with a 100 Hz frequency, 10% duty cycle and 500 ms duration. The voltages ranged from 0.5 to 1.5 V with a step width of 0.1 V. While stimulating the foreleg protraction muscles, the EMG of flight muscles was recorded. Five flight muscles were measured, including the dorso-longitudinal muscle, dorso-ventral muscle, basalar muscle, subalar muscle and second axillary muscle. The minimum voltage that elicited regular EMG spikes on any flight muscle was defined as the threshold. The overall threshold voltage was 0.90±0.07 V (N=5 beetles, n=5 thresholds). Accordingly, the amplitude of all electrical stimulations was set to 0.7 V.

Prior to the free-flight stimulation, induced leg motion was verified on each tethered beetle. Next, the beetle was released into the air, and stimulation commands were transmitted wirelessly. The monophasic square pulse signals were set to 0.7 V, 100 Hz and 10% duty cycle with 500 ms duration. The induced yaw torque by leg motion was evaluated by the flight turning rates (Cheng et al., 2010; Fry et al., 2003). Based on the recorded flight trajectory, the turning rate ω can be calculated from three consecutive positions (P_1, P_2 and P_3) on the horizontal plane as follows:

$$\omega = \cos^{-1}\left(\frac{\overrightarrow{P_1P_2}\cdot\overrightarrow{P_2P_3}}{|\overrightarrow{P_1P_2}|\cdot|\overrightarrow{P_2P_3}|}\right)/\left(\frac{t_{P_3}-t_{P_1}}{2}\right). \quad (3)$$

By synchronizing the flight trajectory with the stimulation commands, the induced turning rate $\omega_{induced}$, given by $\omega_{induced}=\omega_{150}-\omega_0$, where ω_0 and ω_{150} are the turning rates immediately before stimulation and 150 ms after stimulation, respectively, was computed to analyze the stimulation effect. This experiment was completed using intact and amputated beetles. After testing each intact beetle, both forelegs were cut off from the coxae. The above electrical stimulations were repeated on the amputated beetles with the same configuration. The induced turning rates computed from the amputated beetles were compared with the results of intact beetles. For the calculation of induced turning rates, all results greater than 30 deg s^{-1} were excluded from the dataset because this is larger than the possible effect generated by the foreleg.

RESULTS

Once a beetle starts to fly, whether in free or tethered flight, its forelegs extend (Fig. 1). We hypothesized that the unique posture of a beetle may have some effects on its flight control, especially on the turning control. Thus, we conducted leftward and rightward visual stimulation of tethered beetles using optical flow of dark and bright stripes to induce fictive turns (Götz and Wenking, 1973). To study the correlation between turning and foreleg motion, we tracked foreleg motion during visual stimulation using a 3D motion capture system (Vicon; Fig. S1). During the fictive turns, the horizontal swinging of extended forelegs was frequently observed (Fig. 2A). Within a sample size (N=10 beetles, n=80 left fictive turns, n=80 right fictive turns), we found that the forelegs mostly swung clockwise (from the view of the beetle's dorsal side) to produce fictive left turns and counterclockwise to produce fictive right turns (P<0.0001, binomial test; Fig. 2B).

We speculated that the leg swings associated with fictive turns were actively induced by the beetle itself, i.e. visually stimulated beetles exhibit optomotor responses, including the activation of leg muscles, to produce swinging. To clarify whether the leg swings were produced actively or passively, we used EMG to assess the protraction muscle of the left leg (Fig. 3A) during visual stimulation. The contractions of the muscle in the left foreleg cause it to swing clockwise (Cao et al., 2014). Indeed, a one-sample t-test indicated the majority of EMG spikes in the muscle occurred during left fictive turns (N=5 beetles, n=5 EMG recordings, t_4=10.82, P=0.0002; Fig. 3B,C). This result suggests that the foreleg swings during fictive turns (Fig. 2) are not induced by external forces but rather by the tension created by leg muscle contraction.

The yaw torque exerted on a beetle's body during a leg swing effectively rotates the body. We tethered a beetle on a torque meter and electrically stimulated the protraction muscle of the left foreleg to produce clockwise swinging (N=4 beetles, n=40 trials). It is known that the pitch angle mainly correlates with the longitudinal flying speed and does not apparently influence on the horizontal turning on flapping wing flyers (Cheng et al., 2011, 2016). Thus, we focused on the analysis of yaw torque and roll torque. The results revealed that the induced torque in yaw was as much as ∼7 µN m whereas the induced torque in roll was relatively small, ∼2 µN m (Fig. 4Ai,Bi). Meanwhile, the moment of inertia estimated from the beetle model is 12.36 g cm^2 in yaw and 7.73 g cm^2 in roll. Thus, the induced angular displacement was calculated as 1.62 deg in yaw and 0.69 deg in roll within 200 ms. We repeated the same experiment and analysis after removing the legs from the body. The measured torque was smaller, indicating that the significant torque observed prior to leg removal was solely due to foreleg swinging (N=4 beetles, n=40 trials; Fig. 4Aii,Bii).

Moreover, the induced turning rate of trajectory could be simulated based on the leg-induced yaw torque. While the body rotates to induce a flight turning, the centrifugal force of the turning is provided by the misaligned horizontal propulsion, which can be expressed as follows:

$$m\cdot v\cdot\omega_{traj} = F_h\cdot\sin(\theta), \quad (4)$$

where m is the mass of the beetle, v is the horizontal flight velocity, ω_{traj} is the turning rate of trajectory, F_h is the horizontal propulsion and θ is the included angle between body orientation and flight trajectory. As the leg-induced angular displacement is ∼1.6 deg in body orientation, the included angle should be even smaller. Then the equation can be transformed as follows:

$$m\cdot v\cdot\omega_{traj} \approx F_h\cdot\theta = F_h\cdot\left(\int\omega_{body}-\int\omega_{traj}\right), \quad (5)$$

where ω_{body} is the angular velocity of the body. Furthermore, the horizontal propulsion measured by the torque meter from tethered flying beetles was 0.131±0.014 N (N=5 beetles, n=50 measurements). Li et al. (2016) demonstrated that the average flight velocity of a beetle with a backpack loaded was 5.57 m s^{-1}. As the sixth-order polynomial curve fitting was carried out for the induced angular velocity in Fig. 4Ai, the corresponding turning rate of trajectory induced by yaw torque could be solved and the value was 3.84 deg s^{-1} at 150 ms after stimulation.

As further support of the role of forelegs inflight, we demonstrated that exogenous stimulation of the leg muscles induces foreleg swinging and subsequent turning while in free

Journal of Experimental Biology (2017) 220, 3499-3507 doi:10.1242/jeb.159376

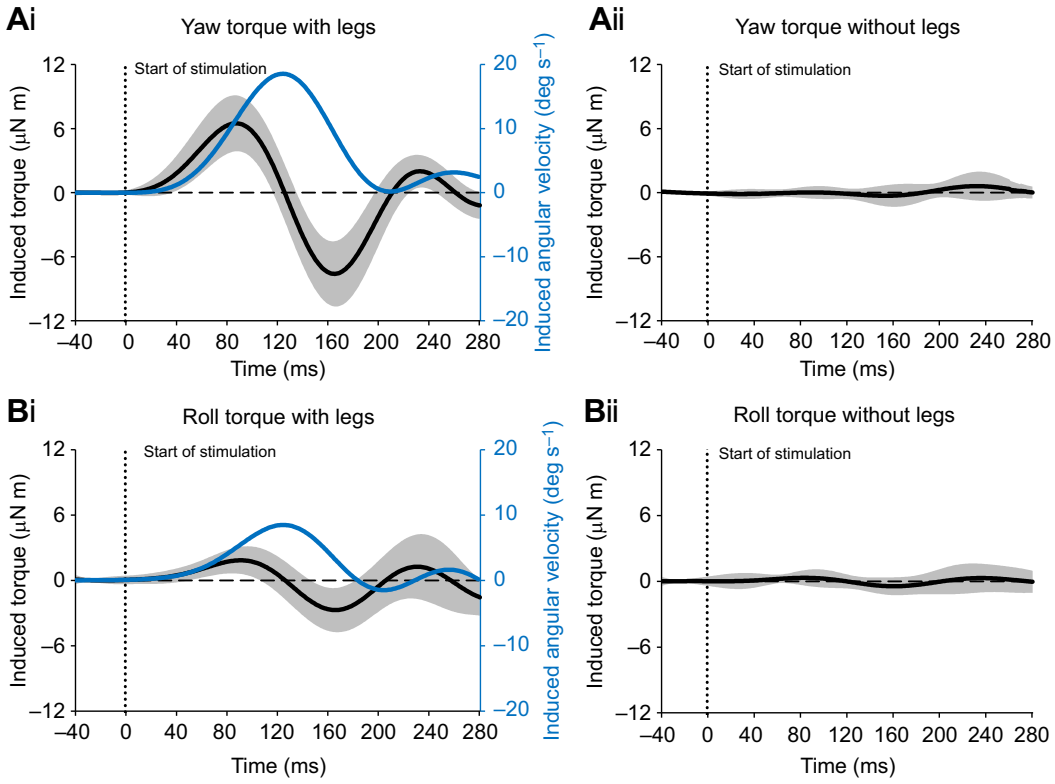

Fig. 4. The induced torque generated by electrical leg stimulation. The induced yaw torque (A) and roll torque (B) on the body, ΔT_{yaw} and ΔT_{roll}, were measured on both intact (Ai,Bi) and amputated (Aii,Bii) beetles by stimulating the left foreleg with 0.7 V electrical pulse signals. The black solid line represents the average induced torque, and the gray shaded area indicates the s.e.m. (N=4 beetles, n=40 trials). The blue lines represent the calculated body angular velocities based on the induced torques.

flight (Fig. S3). A radio-controlled backpack (Fig. S3) was mounted on the beetle, and the protraction muscles of the left and right forelegs were alternatively stimulated to induce the clockwise swing of the left foreleg and the counterclockwise swing of the right foreleg, respectively. As expected during free flight, the beetle turned left when the left foreleg was stimulated to swing clockwise, and vice versa (N=5 beetles, n=162 left stimulations, n=184 right stimulations, P<0.0001, binomial test; Fig. 5B,Ci,Di). Because of the electrical stimulation of left or right foreleg protraction muscle, the mean induced turning rates were 3.29±12.71 and −5.42 ±11.57 deg s^{-1}, respectively (the positive or negative value indicates that the turning rate for left or right turns increases). We confirmed that the electrical stimulation of the protraction muscles solely induced leg swinging and did not affect flight muscles (Fig. S4). Interestingly, once the forelegs were removed from the beetle, left and right turns occurred at a similar rate regardless of which side was stimulated (N=5 beetles, n=90 left stimulations, n=90 right stimulations; Fig. 5Cii,Dii), with mean rates of −0.38 ±12.09 and −2.35±9.60 deg s^{-1}, respectively. According to a t-test, the difference in turning rates between intact and amputated beetles is considered statistically significant under both left (t_{250}=2.23, P=0.013) and right (t_{272}=2.18, P=0.015) electrical stimulations. Thus, the left–right turns shown in Fig. 5Ci,Di were caused by the swinging of the left or right foreleg.

DISCUSSION

In flight, many insects fold their forelegs tightly close to the body, which naturally decreases drag or air resistance, whereas flying beetles stretch out their forelegs for an unknown reason. We hypothesized that the forelegs are ‘intentionally’ outstretched and swung to facilitate turning while inflight and that the beetle turns its body orientation (the direction of propulsion) by swinging its forelegs. To test this hypothesis, we used kinematic and physiological analyses to determine whether swinging the legs during flight was regulated, and we measured the torque exerted on the body during leg swinging using tethered beetles. Furthermore, we induced left and right turns in freely flying beetles by electrically stimulating their leg muscles to produce a swinging motion. This stimulation was achieved by mounting our custom-designed miniature wireless communication device (remote stimulator backpack) on flying beetles.

Through visually inducing fictive turns on tethered beetles, we revealed that the forelegs showed certain swinging motions in accord with the directions of the visual stimulations. Specifically, the beetle voluntarily swings the forelegs clockwise or counterclockwise while inflight to turn in the opposite direction. By monitoring the EMG signals from the left foreleg protraction muscle, whose activation generates a clockwise swing of the left foreleg, we found that the spikes appeared much more frequently in the left visual stimulations than in the right stimulations, which gives the evidence that the swinging motions of forelegs were actively induced by the tension created by muscle contraction rather than passively from some external forces. Thus, beetles voluntarily manipulate their forelegs to produce fictive turns in response to visual stimulation.

Meanwhile, the torque measurement showed that leg swing induced yaw torque on a beetle’s body, which would lead to an angular displacement in yaw of up to 1.62 deg within 200 ms. This finding implies that the torque generated by leg motion is significant enough to rotate the heading direction of the beetle. Because the left

Journal of Experimental Biology (2017) 220, 3499-3507 doi:10.1242/jeb.159376

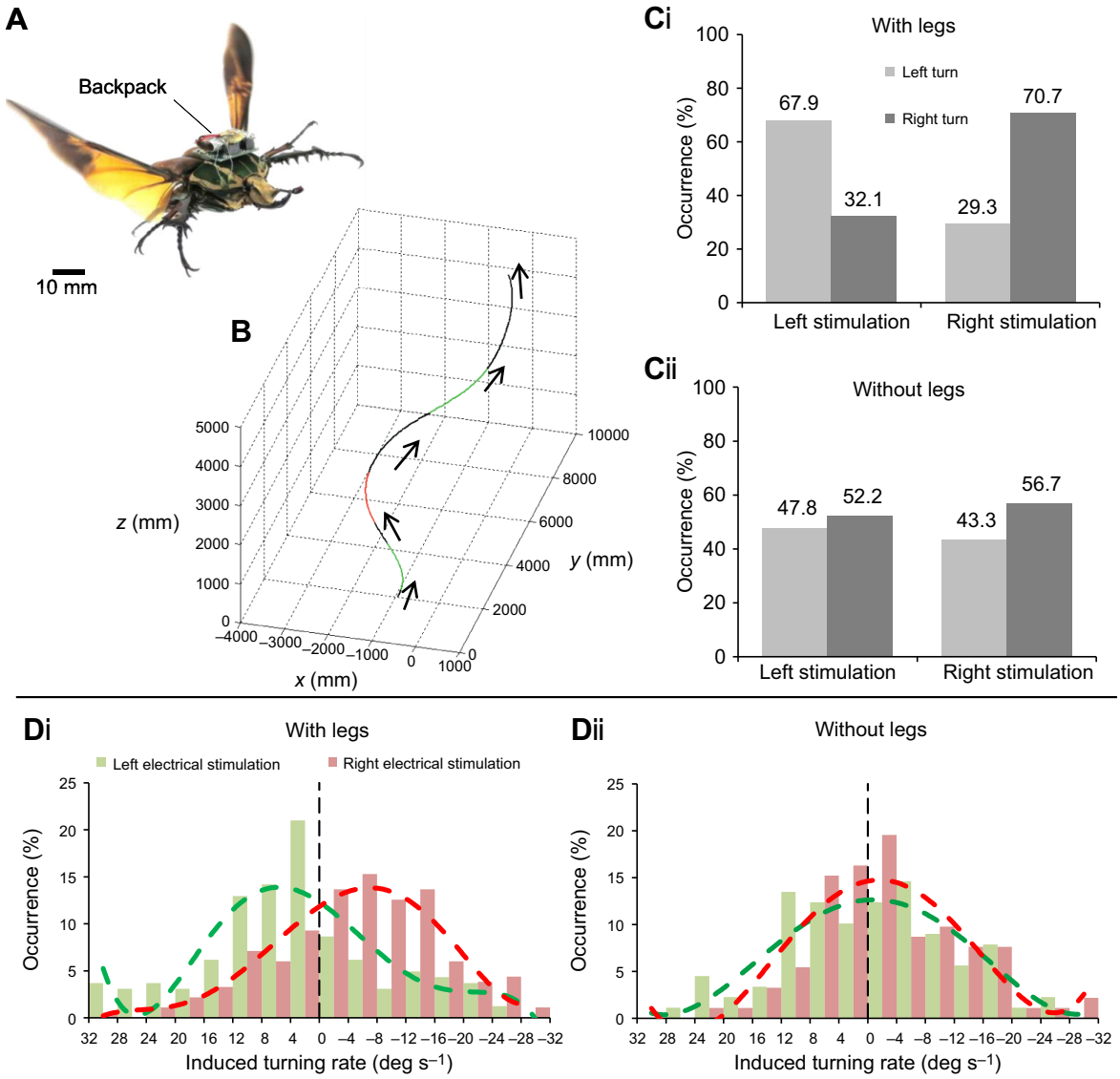

Fig. 5. Responses to electrically stimulated leg motion during free flight. (A) Overview of the backpack-mounted beetle. (B) A zigzag flight path was produced by electrical stimulation of the left (right) foreleg protraction muscle to produce left (right) turns. The electrical stimulation of the left or right protraction muscle induced the swing of the corresponding leg clockwise or counterclockwise (viewed from the dorsal side of the beetle). The black segments indicate the trajectories during non-stimulated periods. Segments in green and red indicate the trajectories during left and right stimulation, respectively. (C) According to the direction of induced turning rate, all stimulation results were categorized into left turn or right turn. The occurrence rates of left and right turns during electrical stimulation were determined before (Ci) and after (Cii) the removal of the legs. Prior to leg removal, left stimulation (clockwise swing of the left foreleg) induced left turns at a rate of 67.9% and right stimulation (counterclockwise swing of the right foreleg) induced right turns at a rate of 70.7% (N=5 beetles, n=162 left stimulations, n=184 right stimulations). These turning rates were significantly different from chance level (P<0.0001, binomial test). After the legs were removed, the occurrence rate was approximately 50% regardless of which side was stimulated (N=5 beetles, n=90 left stimulations, n=90 right stimulations). (D) Histograms of induced turning rates before (Di) and after (Dii) leg removal (negative sign denotes turning toward the right). The green and red dashed lines represent the polynomial fitted distribution of induced turning rates during left and right stimulation, respectively. See Movie 2.

foreleg was stimulated to swing clockwise in the experiment, the body tended to rotate counterclockwise as a consequence. The rotating direction of the body is in accord with the observations in visual stimulation. As a comparison, the induced roll torque would generate a 0.69 deg roll displacement within 200 ms. As a linear relationship between roll angle and yaw angular velocity was found in beetles (Li et al., 2016), the roll displacement (0.69 deg) would correspond to a −2.29 deg s^{-1} angular velocity in yaw, which is smaller than the effect of yaw torque (~13 deg s^{-1}; Fig. 4A). Moreover, the yaw angular velocity induced by clockwise leg swing rotated the body leftwards, which was in accord with the direction of visual stimulation when the forelegs were swinging clockwise. Thus, the leg swing in the turnings should be employed for the yaw turn rather than the bank turn. The use of body posture to change the flying direction by exerting additional torque on the body was previously reported in insects (Berthé and Lehmann, 2015; Zanker et al., 1991). Thus, we believe the beetle swings the forelegs clockwise or counterclockwise in order to generate a yaw torque to rotate its heading direction towards the fictive turns.

The aforementioned findings from the tethered experiments verified our hypothesis that forelegs are swung to facilitate turning. As further support of our hypothesis, we demonstrated that exogenous stimulation of the leg muscles induces foreleg swinging and subsequent turning while in free flight (Fig. S3). In

accord with the results of the tethered experiments, the swinging of the left leg (clockwise) induced a leftward turning and the swinging of the right leg (counterclockwise) induced a rightward turning. After leg amputation, the leftward and rightward turnings showed negligible differences in occurrence rate. The electrical stimulations were exactly applied on the leg protraction muscles without influencing any flight muscles (Fig. S4). These results indicate that the induced turnings are solely because of the swinging motion of forelegs. Moreover, the induced turning rates calculated from the free flights match well with the simulation result based on the yaw torque (3.84 deg s^{-1}), which further verifies that the turnings are induced by the induced yaw torque. As known from visual stimulation that forelegs are voluntarily swung in turnings, we demonstrate that beetles manipulate their forelegs as a mechanism of flight directional control. However, the induced turning rates are relatively small. We understand that the range of leg swing is constrained by the structural limit of the leg coxa and that the leg motion cannot sustain a sharp or long-lasting flight turning. This implies that the forelegs may not be dominant when the beetle is performing sharp turnings. Compared with the wings, the leg motion reveals its advantages in response time and precision. Thus, we believe that the legs serve as a supplementary mechanism to generate small directional corrections or initiate a turning in flight.

It is undeniable that wings, as well as their articulations and flight muscles, are the dominant mechanism for controlling insect flight (Dickinson, 2006; Chapman et al., 2012; Sato et al., 2009, 2015). The operating principles of wings have been well studied in various insects (Zanker et al., 1991; Wang et al., 2003). In fact, beetles flew well even after their legs were removed (Fig. 5Dii). However, the present study indicates that the outstretched foreleg plays a supplemental role in steering during flight. Auxiliary flight control by body parts other than wings has been established in some insects (Baader, 1988; Dyhr et al., 2013; Zanker, 1988; Luu et al., 2011; Camhi, 1970; Combes and Dudley, 2009; Lorez, 1995; May and Hoy, 1990; Hensler and Robert, 1990; Berthé and Lehmann, 2015). For example, flies, locusts and honeybees can sway or twist their abdomen to facilitate turning during flight or change their body posture to adjust their flight speed (Baader, 1988; Dyhr et al., 2013; Zanker, 1988; Luu et al., 2011; Camhi, 1970). The abdomen of a beetle is relatively rigid and short; thus, it maybe not feasible or effective to manipulate the abdomen as a method of steering control during flight (Crowson, 2013; Lawrence and Newton, 1982). The forelegs of beetles are relatively large, wide and thick when compared with those of other insects (Fig. 1); however, this design may not be primarily for steering while flying but rather for direct use, such as dirt digging. If these large legs were folded closely to the body, they would be useless in flight. Instead, the beetles outstretch and swing their forelegs to facilitate turning during flight. In this study, we assessed only the forelegs; however, the middle and hind legs may have a similar function because they are also outstretched while the beetle is flying (Fig. 1). Collectively, future studies on the effect of wings and other non-wing body parts on flight should clarify insect flight mechanisms and provide novel insights for the design of insect-scale robotic flapping flyers.

Acknowledgements
The authors thank Mr Roger Tan Kay Chia, Prof. Low Kim Huat, Mr Chew Hock See and Dr Mao Shixin (Nanyang Technological University) for their support in setting up and maintaining the research facilities. The authors also thank Prof. Michel M. Maharbiz (University of California, Berkeley) for his advice, Prof. Kris Pister and his group (University of California, Berkeley) for their support in providing the wireless devices used in this study, and Mr Kazuo Unno for providing the photographs of flying insects.

Competing interests
The authors declare no competing or financial interests.

Author contributions
Conceptualization: Y.L., H.S.; Methodology: Y.L., F.C., T.V., H.S.; Software: Y.L., T.V.; Validation: Y.L., F.C.; Formal analysis: Y.L., T.V., H.S.; Investigation: Y.L., F.C., H.S.; Writing - original draft: Y.L., H.S.; Writing - review & editing: Y.L., H.S.; Visualization: H.S.; Supervision: H.S.; Project administration: H.S.; Funding acquisition: H.S.

Funding
This study is based on the works supported by a Nanyang Technological University Assistant Professorship (NAP, M4080740) and the Ministry of Education - Singapore (MOE, 2013-T2-2-049, 2015-T1-001-094).

Supplementary information
Supplementary information available online at
http://jeb.biologists.org/lookup/doi/10.1242/jeb.159376.supplemental

References

Arbas, E. A. (1986). Control of hindlimb posture by wind-sensitive hairs and antennae during locust flight. *J. Comp. Physiol. A* **159**, 849-857.
Baader, A. (1988). Some motor neurones of the abdominal longitudinal muscles of grasshoppers and their role in steering behaviour. *J. Exp. Biol.* **134**, 455-462.
Berthé, R. and Lehmann, F.-O. (2015). Body appendages fine-tune posture and moments in freely manoeuvring fruit flies. *J. Exp. Biol.* **218**, 3295-3307.
Borst, A. (1986). Time course of the houseflies' landing response. *Biol. Cybern.* **54**, 379-383.
Burrows, M. (1996). *The Neurobiology of an Insect Brain*. Oxford: Oxford University Press.
Camhi, J. M. (1970). Yaw-correcting postural changes in locusts. *J. Exp. Biol.* **52**, 519-531.
Cao, F., Zhang, C., Vo Doan, T. T., Li, Y., Sangi, D. H., Koh, J. S., Huynh, N. A., Aziz, M. F. B., Choo, H. Y., Ikeda, K. et al. (2014). A biological micro actuator: graded and closed-loop control of insect leg motion by electrical stimulation of muscles. *PLoS ONE* **9**, e105389.
Chapman, R. F., Simpson, S. J. and Douglas, A. E. (2012). *The Insects: Structure and Function*. Cambridge: Cambridge University Press.
Cheng, B., Fry, S. N., Huang, Q. and Deng, X. (2010). Aerodynamic damping during rapid flight maneuvers in the fruit fly *Drosophila*. *J. Exp. Biol.* **213**, 602-612.
Cheng, B., Deng, X. and Hedrick, T. L. (2011). The mechanics and control of pitching manoeuvres in a freely flying hawkmoth (*Manduca sexta*). *J. Exp. Biol.* **214**, 4092-4106.
Cheng, B., Tobalske, B. W., Powers, D. R., Hedrick, T. L., Wethington, S. M., Chiu, G. T. and Deng, X. (2016). Flight mechanics and control of escape manoeuvres in hummingbirds. I. Flight kinematics. *J. Exp. Biol.* **219**, 3518-3531.
Combes, S. A. and Dudley, R. (2009). Turbulence-driven instabilities limit insect flight performance. *Proc. Natl Acad. Sci. USA* **106**, 9105-9108.
Crowson, R. A. (2013). *The Biology of the Coleoptera*. Cambridge, MA: Academic Press.
Dickinson, M. (2006). Insect flight. *Curr. Biol.* **16**, R309-R314.
Dyhr, J. P., Morgansen, K. A., Daniel, T. L. and Cowan, N. J. (2013). Flexible strategies for flight control: an active role for the abdomen. *J. Exp. Biol.* **216**, 1523-1536.
Fry, S. N., Sayaman, R. and Dickinson, M. H. (2003). The aerodynamics of free-flight maneuvers in *Drosophila*. *Science* **300**, 495-498.
Götz, K. G. and Wenking, H. (1973). Visual control of locomotion in the walking fruitfly *Drosophila*. *J. Comp. Physiol.* **85**, 235-266.
Hensler, K. and Robert, D. (1990). Compensatory head rolling during corrective flight steering in locusts. *J. Comp. Physiol. a-Neuroethol. Sens. Neural Behav. Physiol.* **166**, 685-693.
Lawrence, J. F. and Newton, A. F. (1982). Evolution and classification of beetles. *Annu. Rev. Ecol. Syst.* **13**, 261-290.
Li, Y., Cao, F., Thang Vo Doan, T. and Sato, H. (2016). Controlled banked turns in coleopteran flight measured by a miniature wireless inertial measurement unit. *Bioinspir. Biomim.* **11**, 056018.
Lorez, M. (1995). Neural control of hindleg steering in flight in the locust. *J. Exp. Biol.* **198**, 869-875.
Luu, T., Cheung, A., Ball, D. and Srinivasan, M. V. (2011). Honeybee flight: a novel 'streamlining' response. *J. Exp. Biol.* **214**, 2215-2225.
Manecy, A., Marchand, N., Ruffier, F. and Viollet, S. (2015). X4-MaG: a low-cost open-source micro-quadrotor and its linux-based controller. *Int. J. Micro Air Vehicles* **7**, 89-109.
May, M. L. and Hoy, R. R. (1990). Leg-induced steering in flying crickets. *J. Exp. Biol.* **151**, 485-488.
Miall, R. C. (1990). Visual control of steering in locust flight – the effects of head movement on responses to roll stimuli. *J. Comp. Physiol. a-Sensory Neural Behav. Physiol.* **166**, 735-744.

Journal of Experimental Biology

Mountcastle, A. M., Ravi, S. and Combes, S. A. (2015). Nectar vs. pollen loading affects the tradeoff between flight stability and maneuverability in bumblebees. *Proc. Natl Acad. Sci. USA* **112**, 10527-10532.
Nachtigall, W. (1974). *Insects in Flight: A Glimpse Behind the Scenes in Biophysical Research*. New York: McGraw-Hill Companies.
Rowell, C. H. F. (1988). Mechanisms of flight steering in locusts. *Experientia* **44**, 389-395.
Sato, H., Berry, C. W., Peeri, Y., Baghoomian, E., Casey, B. E., Lavella, G., Vandenbrooks, J. M., Harrison, J. F. and Maharbiz, M. M. (2009). Remote radio control of insect flight. *Front. Integr. Neurosci.* **3**, 24.
Sato, H., Vo Doan, T. T., Kolev, S., Huynh, N. A., Zhang, C., Massey, T. L., Van Kleef, J., Ikeda, K., Abbeel, P. and Maharbiz, M. M. (2015). Deciphering the role of a coleopteran steering muscle via free flight stimulation. *Curr. Biol.* **25**, 798-803.
Taylor, G. K. and Thomas, A. L. R. (2003). Dynamic flight stability in the desert locust *Schistocerca gregaria*. *J. Exp. Biol.* **206**, 2803-2829.
Thies, S. B., Tresadern, P., Kenney, L., Howard, D., Goulermas, J. Y., Smith, C. and Rigby, J. (2007). Comparison of linear accelerations from three measurement systems during “reach & grasp”. *Med. Eng. Phys.* **29**, 967-972.
Van Truong, T., Byun, D., Lavine, L. C., Emlen, D. J., Park, H. C. and Kim, M. J. (2012). Flight behavior of the rhinoceros beetle *Trypoxylus dichotomus* during electrical nerve stimulation. *Bioinspir. Biomim.* **7**, 036021.
Van Truong, T., Le, T. Q., Park, H. C., Yoon, K. J., Kim, M. J. and Byun, D. (2014). Non-jumping take off performance in beetle flight (rhinoceros beetle *Trypoxylus dichotomus*). *J. Bionic Eng.* **11**, 61-71.
Wagner, H. (1986). Flight performance and visual control of flight of the free-flying housefly (*Musca domestica* L).1. Organization of the flight motor. *Philos. Trans R. Soc. Lond. B.Biol, Sci.* **312**, 527-551.
Wang, H., Zeng, L., Liu, H. and Yin, C. (2003). Measuring wing kinematics, flight trajectory and body attitude during forward flight and turning maneuvers in dragonflies. *J. Exp. Biol.* **206**, 745-757.
Zanker, J. M. (1988). How does lateral abdomen deflection contribute to flight control of *Drosophila melanogaster*? *J. Comp. Physiol. A* **162**, 581-588.
Zanker, J. M., Egelhaaf, M. and Warzecha, A.-K. (1991). On the coordination of motor output during visual flight control of flies. *J. Comp. Physiol. A* **169**, 127-134.

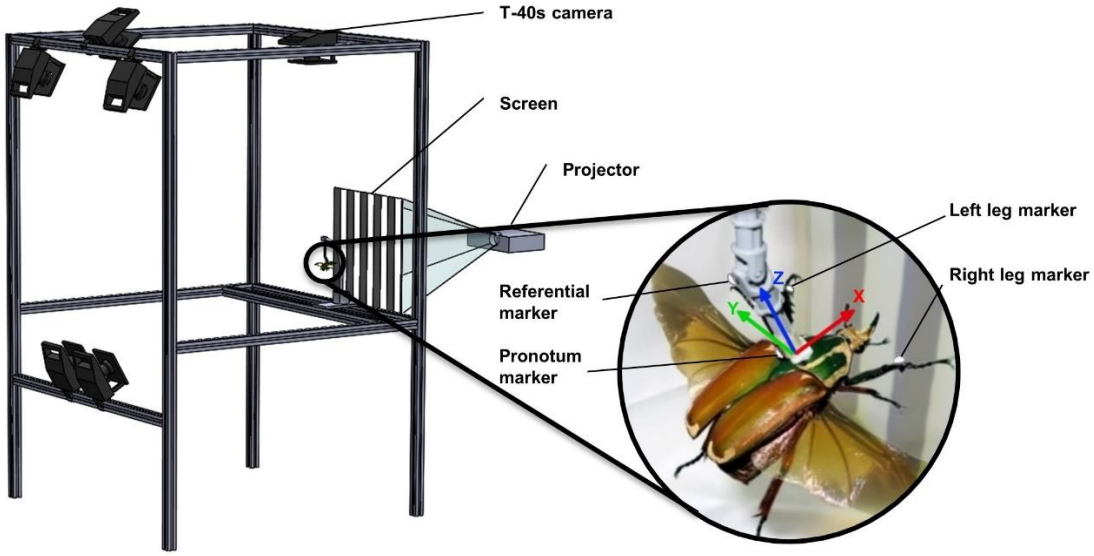

Fig. S1. The configuration of visual stimulation. In visual stimulation, a projector and a transparent screen were used to present the optical flow, and six T40s cameras were used to track leg positions. The beetle was suspended under a universal coupler, and four retro-reflective markers were placed onto the beetle. Two leg markers were placed at the tips of both tibias, the pronotum marker was placed at the posterior end of the pronotum, and a referential marker was placed at the rotation center of the coupler.

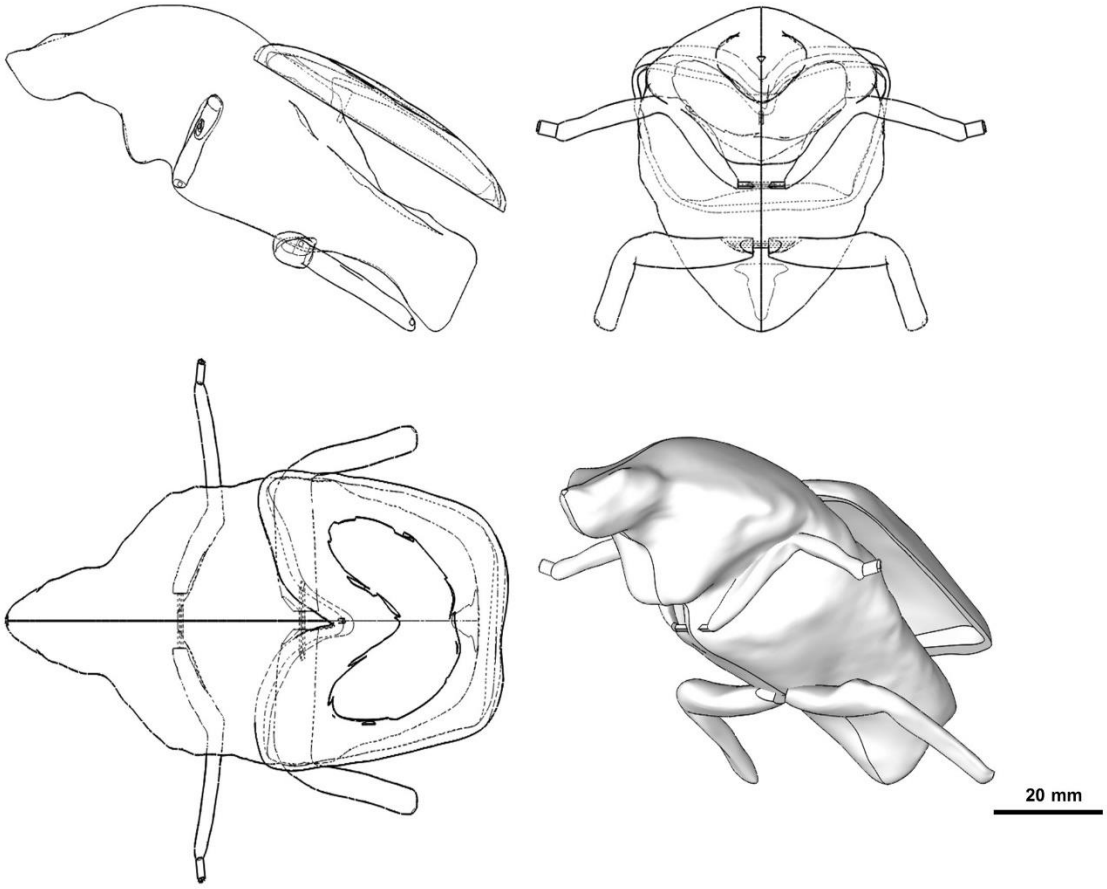

Fig. S2. The scanned 3D beetle model. The front view, left view, top view and oblique view of the model was shown in upper left, upper right, lower left and lower right, respectively. A beetle was scanned with a 3D scanner (EinScan-Pro, Shining 3D; 0.05 mm accuracy). The scanned point-cloud model was digitalized in 3D modelling software (SolidWorks 2016, Dassault Systemes) in 1:1 ratio with the real beetle. The weights of pronotum, abdomen, elytra and legs were separately measured from real beetles (N = 5 beetles) and input into the beetle model.

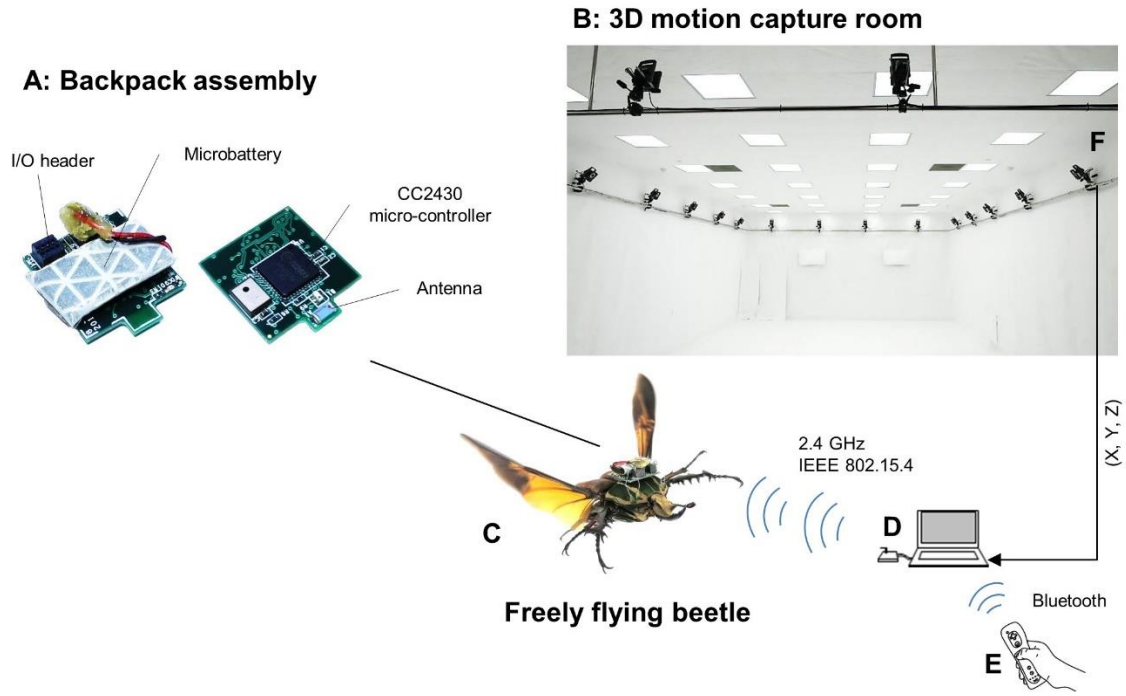

Fig. S3. (A) Photographs of the top and bottom of the wireless backpack assembly (dimensions: 16 × 16 mm^2; mass of the circuit board = 690 mg, mass of the circuit board + battery = 1351 mg). The assembly contained a micro-controller-based circuit board (CC2430, 7 × 7 mm^2, 130 mg, 32 MHz clock, 2.4 GHz IEEE802.15.4-compliant RF transceiver, Texas Instruments) and a rechargeable lithium ion battery (3.7 V, 350 mg, 8.5 mAh; Micro Avionics). The surface was wrapped with retro-reflective tape (Silver-White, Reflexite) to enable detection by the installed cameras shown in (B). **(B)** The experiment was conducted in a flight arena of 12 × 8 × 4 m^3 equipped with a motion capture system of 20 near-infrared cameras (Vicon, T40s and T160). **(C)** The backpack was assembled and mounted onto the beetle before releasing the beetle into the air for free flight. The backpack received wireless signals from a laptop **(D)** equipped with a base station when the operator pressed the command button of the Wii remote **(E).** On command, the backpack applied an electrical stimulus to the foreleg muscles. The coordinates of the flying beetle were recorded with timestamps by the motion capture system **(F).** These coordinates were sent to the laptop for synchronization with the stimulation command.

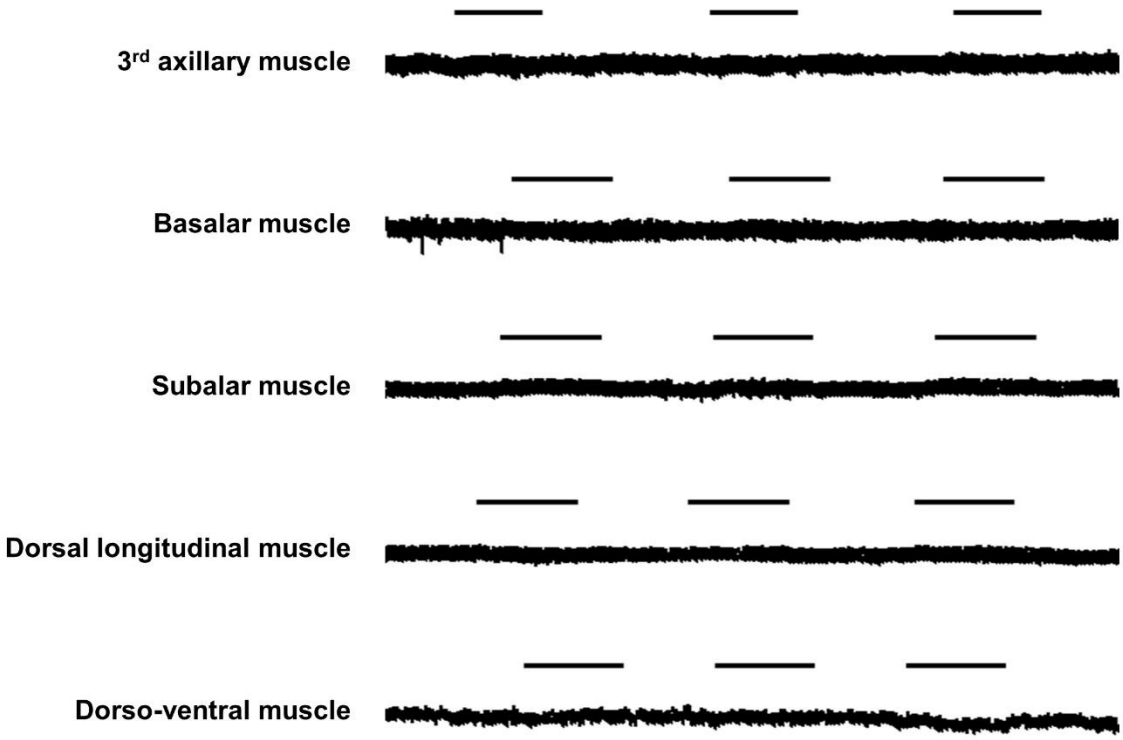

Fig. S4. EMG of flight muscles during electrical leg stimulation. The stimulation consisted of 0.7 V pulses for 500 ms (black bars). The electrical stimulation of leg muscle caused no clear EMG spikes on the flight muscles (N = 5 beetles, n = 50 stimulations), which suggests that the electrical leg stimulation does not influence flight muscles.

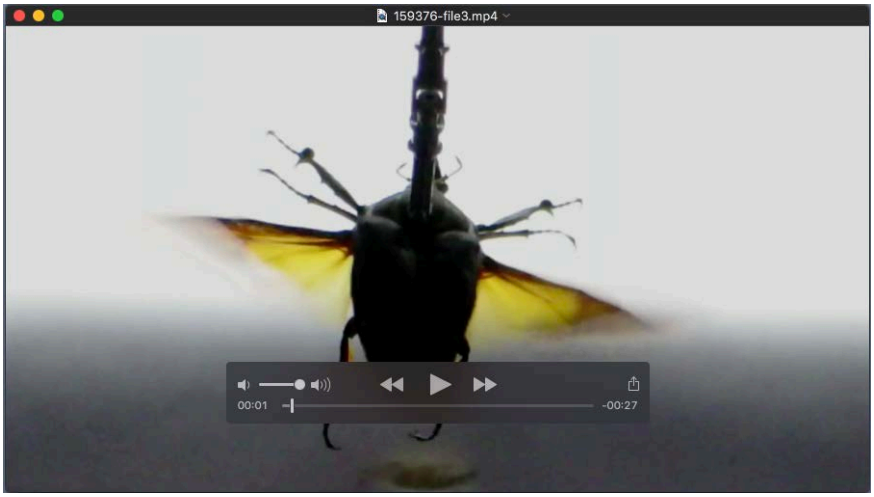

Movie 1. The forelegs of beetle revealed regular motion patterns along with the leftward and rightward visual fictive turnings. The camera was placed 15 cm behind the beetle recording in a 60 degree downward view. The period of visual stimulation was 5 s and the period between two stimulations was 2 s. During fictive left turnings (strips moving leftwards), the left leg moved closer to the body and the right leg moved away from the body (clockwise). During fictive right turnings (strips moving rightwards), right leg moved closer to the body and the left leg moved away from the body (counterclockwise).

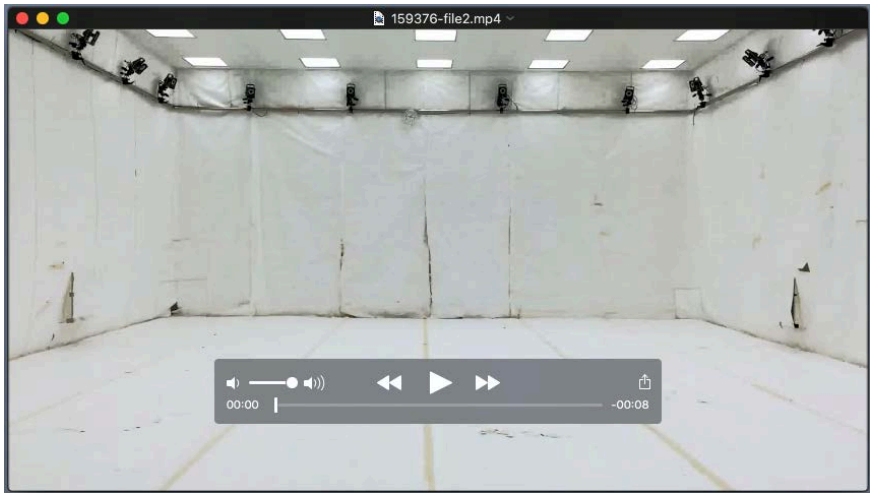

Movie 2. A freely flying beetle displayed left and right turns as a result of the left and right foreleg swinging induced by electrical stimulation of the protraction muscles. The stimulation of the left foreleg protraction muscle induced a clockwise (viewed from the dorsal side of the beetle) swing of the left foreleg and resulted in a left turn of the beetle. The same set of unilateral responses occurred with right stimulation. High and low tone sounds indicated the timing of the left and right foreleg stimulations, respectively. The latter half of the movie shows the animated flight path reconstructed from the data acquired using the 3D motion tracking system. Green and red flight paths correspond to the timing of the left and right foreleg stimulations, respectively.

Journal of Experimental Biology • Supplementary information